

Solid-Core Photonic Bandgap Fibers for High-Power Fiber Lasers

Evgeny M. Dianov, *Member, IEEE*, Mikhail E. Likhachev, and Sébastien Février

(Invited Paper)

Abstract—An overview of various designs of large-mode-area photonic bandgap fibers (PBGFs) is presented in this paper. Bending properties of these structures are discussed and compared with those of step-index and air-silica microstructured fibers. Peculiarities of active PBGF fabrication are considered, and novel high-power laser architecture based on such fibers is described.

Index Terms—Optical fiber lasers, optical fibers.

I. INTRODUCTION

HIGH-POWER continuous-wave (CW) and pulsed fiber lasers are of great interest owing to their high reliability, diffraction-limited beam quality, and high pump-to-signal conversion efficiency. The main factor limiting the output power at the level of 1 kW in the CW regime and the peak power at the level of 100 kW in the picosecond-pulse regime is the appearance of nonlinear effects in the fibers used as the active medium in such lasers. Stimulated Brillouin or Raman scattering as well as four-wave mixing drastically reduces the efficiency of the lasers and severely alters the spectral beam quality. To increase the threshold of appearance of nonlinear effects, large-mode-area (LMA) fibers are currently used. An increase in the active core diameter has also another advantage: it allows one to increase the pump absorption in the double-clad configuration, shorten the active fiber length, and thus further increase the threshold of the nonlinear effects.

By nature, the LMA architecture is obtained at the expense of weakening waveguidance in the fiber, leading to strong bend sensitivity. Step-index LMA fibers provide single-mode regime only with core diameter $D \leq 25 \mu\text{m}$ at $\lambda = 1.08 \mu\text{m}$ (the emission wavelength of Yb^{3+} ions) [1]. Endlessly, single-mode photonic crystal fibers (PCFs) are also employed [2]. The core diameter can be increased to $40 \mu\text{m}$, but propagation in this case is slightly multimode [3]. Recently, PCF with a core diameter of $80 \mu\text{m}$ and a laser based on such fibers with a very good spatial beam quality ($M^2 < 1.2$) were demonstrated [4]. In these cases, curvature loss became extra high and required the use of absolutely straight fibers (so-called rod-type fibers), making the

laser somewhat cumbersome. Moreover, PCF with such high core diameters cannot be spliced with other fibers; therefore, pump input and signal input/output are realized by volume elements. The necessity to align the fiber in the laser assembly results in losing reliability of the device.

For this reason, much attention is now paid to the investigation of new waveguide structures with a low bend sensitivity and an increased core size. For example, LMA multimode step-index fibers allow achieving single-modedness and a very good spatial beam quality ($M^2 < 1.1$) owing to high-order mode filtering. The latter is obtained by appropriate fiber curvature [5]. A simple holey fiber consisting of a solid core surrounded by a single ring of large holes has also proved to be a good candidate [6]. Utilization of high-order modes [7], or their suppression by a microstructured cladding [8] allows gaining bend resistance in step-index fibers. Helical-core fibers [9], spun-double-core fibers [10], or gain-guided, index-antiguidded fibers [11] are also promising designs.

In this paper, we discuss novel high-power laser architectures based on utilization of solid-core photonic bandgap fibers (PBGFs). Propagation in such fibers relies on the Fresnel reflection of light from a microstructured periodic cladding surrounding the core. Because light propagation in PBGF is not due to total internal reflection, the core index can be lower than that of the surrounding cladding. The cladding exhibits either 1-D or 2-D periodicity. The 1-D structures, so-called Bragg fibers [12], consist of a low-index core surrounded by alternating high- and low-index rings. The 2-D structure involves high-index cylinders in hexagonal package surrounding a low-index core [13].

II. DESIGN OF LMA SOLID-CORE PBGF

Since the first proposition in 1978 by Yeh *et al.* [12], PBGFs have been widely studied for their unusual properties, such as the possibility of dispersion management [14], [15] and tailoring the emission spectrum in laser applications [16], [17]. Such structures are not single mode in the general sense [18], but they allow efficient mode filtering even in the LMA case (the optical loss of different modes can differ by a few orders). Several designs of LMA fibers based on both 1-D and 2-D symmetries have been proposed. Next, we discuss the properties and advantages of the various designs.

A. 1-D Structure (Bragg Fiber), $D = 22\lambda$

The first LMA PBGF structure proposed was based on the 1-D design [19] and had a core diameter 22λ (λ is the working

Manuscript received October 1, 2008; revised October 30, 2008; accepted October 30, 2008. Current version published February 4, 2009.

E. M. Dianov and M. E. Likhachev are with the Fiber Optics Research Center, Russian Academy of Sciences, Moscow 119333, Russia (e-mail: likhachev@fo.gpi.ru).

S. Février is with Xlim, Unités Mixtes de Recherche (UMR) 6172 Centre National de la Recherche Scientifique (CNRS), University of Limoges, Limoges 87060, France (e-mail: sebastien.fevrier@xlim.fr).

Color versions of one or more of the figures in this paper are available online at <http://ieeexplore.ieee.org>.

Digital Object Identifier 10.1109/JSTQE.2008.2010247

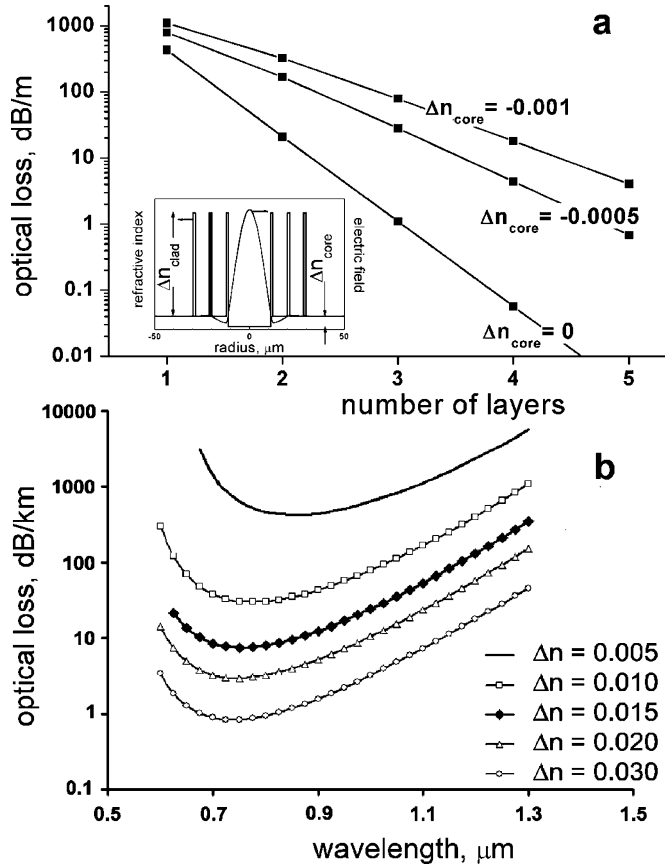


Fig. 1. (a) Optical loss in fibers with different Δn_{core} and different number of high-index layers in the cladding. (b) Optical loss calculated for the fibers with $\Delta n_{\text{core}} = 0$, three high-index layers, and different Δn_{clad} . Refractive index differences Δn_{core} and Δn_{clad} are calculated relative to the outer silica cladding level.

wavelength). High propagation loss (~ 1 dB/m) revealed in such a fiber was due to inaccuracy of the refractive index profile (RIP) and a small difference in the index of the cladding layers (~ 0.005). Optimization of this structure is of primary interest because background loss will severely limit the net gain and efficiency in fiber laser or amplifier. Next, we discuss an improved design of LMA Bragg fibers with a core diameter of 22λ and a low confinement loss proposed in [20].

The fundamental HE_{11} mode can be tightly confined in the low-index core of the Bragg fiber at a specified wavelength by carefully choosing the thicknesses of the high- and low-index layers. They should be equal to one-quarter of the transverse wavelength of the desired guided mode to have minimum optical loss [12]. Optical losses calculated using a standard 1-D solver for the scalar wave equation for such Bragg fibers with a core $D = 24 \mu\text{m}$ are shown in Fig. 1. It can be seen from Fig. 1(a) that a negative Δn_{core} is undesirable if we are looking for the lowest loss design. A positive Δn_{core} results in a reduction of the confinement loss down to zero (at $\Delta n_{\text{core}} = 4 \times 10^{-4}$, the fundamental HE_{11} Bragg mode becomes index guiding) [20]. However, special care should be taken in this case, because at $\Delta n_{\text{core}} = 9 \times 10^{-4}$, the second TE_{01} Bragg mode also becomes index guiding and the fiber will be bimode. Choosing $\Delta n_{\text{core}} = 0$ seems to be the most optimal if we want to guarantee single-

mode low-loss propagation. Further confinement loss reduction is possible by increasing the number of cladding layers [see Fig. 1(a)], or by increasing Δn_{clad} [see Fig. 1(b)]. Increasing the number of the high-index layers results in a growth of the Bragg structure size and complication of the fabrication process. For this reason, it is preferable to change high-index layer's refractive index. An increase of Δn_{clad} from 0.005 to 0.015 decreases the optical loss almost by two orders of magnitude. Further loss reduction is limited in this structure. The reason is that PBGFs are not single mode in the general sense [18], and optical losses of high-order modes do not exceed 10 dB/m in the design with $\Delta n_{\text{clad}} = 0.015$. As a result, the proposed Bragg fiber will reveal single-mode properties only if it is longer than a few meters. An increase of Δn_{clad} results in a simultaneous decrease of the optical loss of the fundamental HE_{11} mode and high-order modes. When Δn is equal to 0.030, the losses of high-order modes become less than 1 dB/m, and such a fiber will be multimode over a length of few meters.

The preform of the Bragg fiber in accordance with the design with $\Delta n_{\text{clad}} = 0.015$ was fabricated by the conventional modified chemical vapor deposition (MCVD) method [20]. Outside of the third high-index ring, a depressed circular layer was added to reduce the bend sensitivity [19]. The RIP of the resultant fiber measured by S14 York fiber analyzer is shown in Fig. 2(a). First of all, single-modedness of the fabricated fiber was verified. Two fiber samples, 1 and 30 m in length, were studied. Light was coupled to the fiber by an ordinary step-index single-mode fiber. The single-mode fiber could be shifted across the Bragg fiber to excite high-order modes. The short sample (1 m length) showed a bimode behavior. The TE_{01} mode was clearly seen in this sample. At the same time, the long sample (30 m length) was single mode—no change in the field distribution was observed when shifting the single-mode fiber. The measured and calculated electric field intensities of the HE_{11} mode are presented in Fig. 2. The mode-field diameter of this mode was $18.5 \mu\text{m}$ at the $1/e$ level and mode-field area equalled $270 \mu\text{m}^2$.

Optical loss was measured by the standard cutback technique. To remove light from the high-index rings, both the ends of the fiber were spliced to ordinary single-mode step-index fibers. The optical loss measured in the 30-m-long fiber wound on a reel 20 cm in radius is presented in Fig. 2(b). It does not exceed 10 dB/km at $\lambda = 1.064 \mu\text{m}$. Further investigations have shown that this loss value is caused mainly by bending losses. The optical loss in the straight fiber was found to be significantly lower. Because of a short fiber length (~ 6 m), only a part of spectrum in the range $1.4\text{--}1.6 \mu\text{m}$ was measured. Estimation of the optical loss in the straight fiber at $1.064 \mu\text{m}$ shows that it is less than 1 dB/km. This small level of optical loss is caused by an additional depressed layer beyond the Bragg mirror and a small depression ($\sim 2 \times 10^{-4}$) of the low n layers [20].

In a cylindrically symmetric Bragg fiber, an even Bragg mode can couple to even modes only. For instance, ring waveguides support even modes. Since the core exhibits the same refractive index as the medium surrounding the rings, these modes are excited near their cutoff. As a consequence, coupling between even modes yields high attenuation peaks associated with the edges of the bandgaps. In a practical situation, however, cylindrical

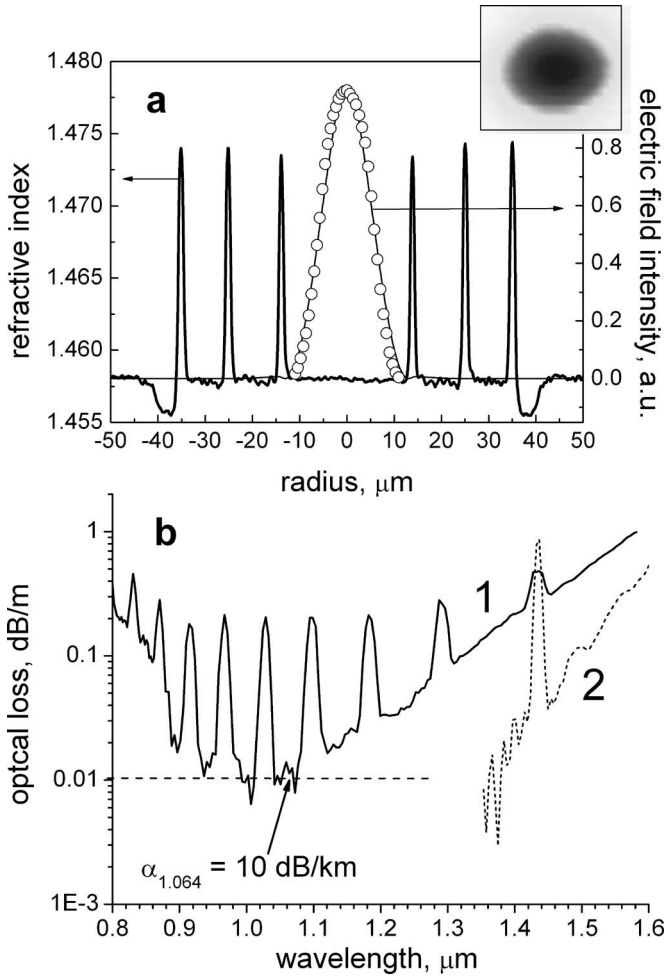


Fig. 2. (a) RIP of a Bragg fiber with core diameter of $D = 22\lambda$ and calculated (line) and measured (dot) electric field intensity distribution of the HE_{11} mode; inset: photograph of near-field distribution. (b) Optical loss for a bend with a radius 20 cm (1) and in a straight Bragg fiber (2).

symmetry of the fiber may be broken, thereby allowing coupling between the Bragg mode and odd modes of the ring waveguides referred to as $LP_{l,m}$ modes (with nonzero azimuthal index l). For a given m index, these modes appear at wavelengths shorter (longer) than the $LP_{0,m}$ ($LP_{0,m+1}$) cutoff wavelengths, respectively. Similar to $LP_{0,m}$ modes, odd modes are excited near their cutoff. Therefore, bending-induced coupling, for instance, yields additional loss peaks within the bandgap (in the fiber presented in Fig. 2, such peaks are situated at 1.027, 1.099, 1.183 μm , etc.). Obviously, the overlap integral between the fields of odd and even modes is rather small, thereby leading to a loss level much lower than that observed in the vicinity of the bandgap edges. It should be noted that this resonant coupling occurs when the effective indexes of the Bragg mode and the $LP_{l,m}$ ring modes become very close to each other. As will be seen next, down doping of the core by only 0.001 suppresses this effect and no sharp loss peaks appear in this case.

B. 1-D Structure (Bragg Fiber), $D = 46\lambda$

Optical loss of the Bragg mode decreases with increasing the core diameter as $1/D^3$ [18] if the parameters of the Bragg

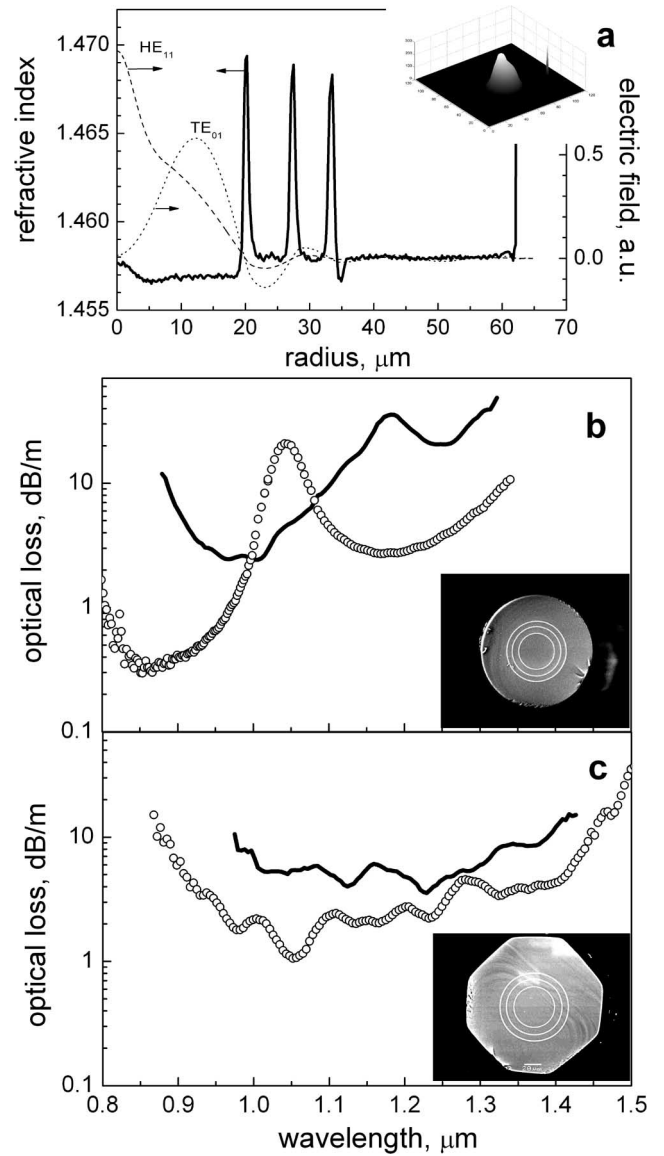


Fig. 3. (a) RIP of the Bragg fiber with a core of $D = 46\lambda$ and a calculated electric field distribution of the HE_{11} and TE_{01} modes; inset: photograph of the near-field distribution for the HE_{11} mode. (b) Optical loss in the Bragg fiber with a circular cladding (dots—straight fiber, line—coiled fiber with radius of 20 cm), inset: SEM image of the fiber. (c) Optical loss in the Bragg fiber with an octagon-shaped cladding (the shift to the longer wavelengths is caused by the 15% increase of the core diameter compared to the circular-cladding Bragg fiber), inset: SEM image of the fiber.

mirror (the number and refractive index of the high-index layers) remain the same. This fact simplifies realization of the fiber with a depressed core index. The design of such a fiber with a core diameter of 46λ was proposed and realized in [21]. The RIP in the fabricated fiber together with the calculated electric field intensity distribution is shown in Fig. 3(a). It can be seen that even a small index step in the core significantly distorts the field pattern and makes it different from the Bessel distribution typical for a flat core. The mode-field area was estimated as $530 \mu\text{m}^2$ at $\lambda = 0.833 \mu\text{m}$. The optical loss measured in the straight fiber and a bent fiber with a radius 20 cm is presented in Fig. 3(b). Instead of one wideband, we observe two loss minima in the spectrum. They arise from interference in the thick outer silica

cladding lying between two good reflectors: the Bragg mirror and the polymer coating (the refractive index of the polymer is typically ~ 1.52 ; therefore, Fresnel reflection from the silica–polymer interface is high) [22]. This effect was not observed in the Bragg fiber shown in Fig. 2(a). It can be shown using the formulas derived in [22] that the optical thickness of the outer silica cladding does not change with wavelength if the core refractive index is equal to that of the outer silica cladding. For this reason, no spectral modulation was observed in this case. Under bending, the minima in the depressed core Bragg fiber become slightly higher and shifted to longer wavelengths. This is caused by an increased angle between the outgoing light beam and the fiber axis in the bent fiber that increases the transparency of interfaces and changes the optical path inside the outer silica cladding. The effect of polymer coating can be suppressed by octagonal shaping of the outer cladding [see Fig. 3(c)] [22].

It is worth noting that in the depressed core design, there are no sharp loss peaks caused by coupling between the Bragg mode and the inner ring mode. As a result, the octagon-shaped fiber possesses the widest low-loss band ever reported for the Bragg fiber. This feature is desirable because it allows using the same fiber for different working wavelengths. Moreover, the exact positions of the loss peaks due to resonant coupling and interference with polymer coating are hard to predict. Typically, a few fibers with close diameters should be fabricated to obtain a low-loss band at the given working wavelength if these two effects are not suppressed. A weak point of the octagon-shaped fiber with a depressed core index is poor single-modedness (the loss ratio of TE_{01} and HE_{11} modes is about 10). As a result, optical loss of the fundamental HE_{11} mode should be kept at a rather high level of ~ 1 dB/m to have single-mode propagation over a few meters fiber length.

Improvement of the single-modedness in the fiber design with core diameter of about 40λ can be achieved by using a pure silica core ($\Delta n_{\text{core}} = 0$). The latest study [23] showed that an additional gain in single-modedness is possible by increasing the optical thickness of the low-index layers relative to one-quarter of the transverse wavelength. In this case, the optical loss of the lowest loss high-order TE_{01} mode grows faster than the loss of the fundamental HE_{11} mode. The optical loss ratio between the TE_{01} and HE_{11} modes exceeds two orders of magnitude in this case.

C. 2-D Structure, $D \sim 21\lambda$

Positions of the bandgaps in solid-core PBGF are defined by the properties of high-index inclusions constituting the cladding (rings in the 1-D case and cylinders in the 2-D case), which can be considered as complex Fabry–Perot resonators. The resonance wavelengths (maximum transmission through the cladding) of these resonators coincide with the cutoff wavelengths of the eigenmodes of the inclusions [24]. For this reason, low-loss transmission bands are situated between the cutoff wavelengths of the high-index inclusions. Whereas the Bragg fibers discussed earlier work in the fundamental band (at the wavelengths higher than the cutoff of the LP_{02} inner ring’s mode [25]), 2-D PBGFs usually operate in high-order

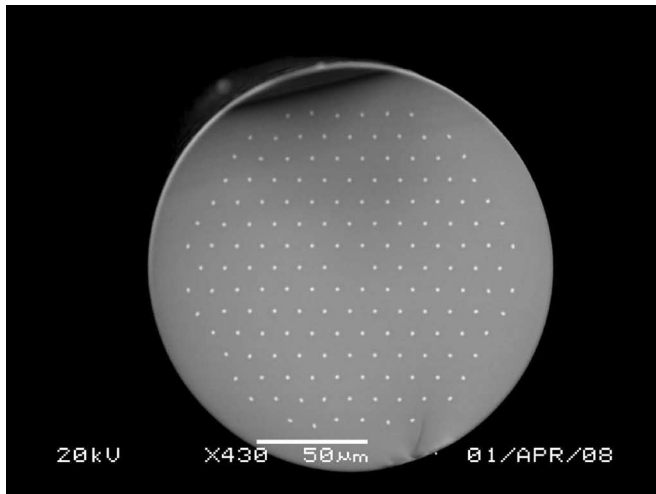
bands. The first demonstration of low-loss propagation in solid-core PBGF was made for a fiber operating in the third-order band [26]. The fiber had a core diameter $D = 20 \mu\text{m}$ and guided light near $1.55 \mu\text{m}$ ($D = 13\lambda$). The optical losses less than 20 dB/km were obtained by using seven periods of high-index rods. The outer diameter of the fiber was $300 \mu\text{m}$. The d/Λ ratio (d is the diameter of the high-index inclusion and Λ is the distance between their centers) was about 0.68. One of the advantages of this structure is good single-modedness—no high-order modes were observed in fiber samples longer than 60 cm.

An increase of the core diameter is possible in this design by increasing the band order or by decreasing the refractive index of the inclusion and keeping its cutoffs at constant wavelengths. However, both ways are inefficient. In the first case, narrowing of the low-loss bands and an increase of the bend sensitivity [27] are expected. In the second case, outer diameter will grow together with an increase of the core diameter (the outer diameter is too big even for the structure with $D = 13\lambda$). Adding of one more period of holes beyond the photonic bandgap structure allows a significant reduction of the confinement losses [28]. Decreasing the number of periods and the outer diameter is possible in this case. A drawback of a structure with air holes is deterioration of the single-modedness (the ratio of the losses of the high-order modes and the fundamental mode is about 100 with the same core diameter).

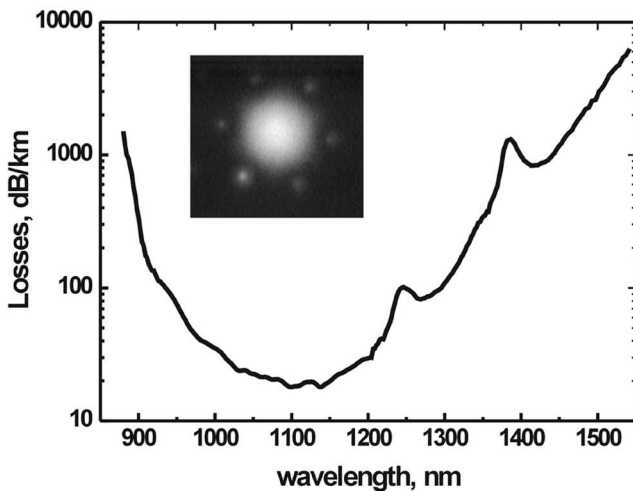
Recently, a new design of the 2-D PBGF based on light guidance in the fundamental band was proposed [29]. Fiber with core diameter of $\sim 23 \mu\text{m}$ working at wavelengths near $1.1 \mu\text{m}$ (core diameter $D = 21\lambda$) was demonstrated [see Fig. 4(a)]. Operation in the fundamental band was achieved by choosing a small d/Λ ratio (0.12 in this design). Despite the fact that the area of the high-index cylinders is very small (as compared to the design published in [26]), the fiber confines light in the core very efficiently. In this case, seven periods of high-index inclusions are enough to have a low propagation loss. It does not exceed 20 dB/km when the fiber is coiled with a radius of 15 cm [see Fig. 4(b)]. A similar result was obtained for the fiber with the large d/Λ ratio reported in [26]. Calculations show that the optical loss of the second mode exceeds 100 dB/m, and no high-order modes were observed even in 10-cm-long fiber samples. A further increase in the core size, up to 32λ , is possible with such a structure [30].

D. Bend Loss in the Solid-Core PBGF

At the beginning of this paper, we emphasized that the bend loss is the most critical factor for the LMA structure. It is interesting to compare the bend sensitivity of PBGF discussed here with the conventional step-index and microstructured fibers. Structures with a mode-field diameter of about $19 \mu\text{m}$ and single mode (or asymptotically single mode in the case of PBGF) at the working wavelength were compared: the Bragg fiber with core $D = 22\lambda$ [20] (see Fig. 2), the 2-D solid-core PBGF with a core diameter of 21λ [29] (see Fig. 4), a step-index fiber operating near the cutoff ([20], see Fig. 5 inset), and an LMA PCF with hole-to-hole spacing $\Lambda = 15 \mu\text{m}$, hole diameter $d = 6.6 \mu\text{m}$ ($d/\Lambda = 0.44$ for single-mode operation), and eight rings of



(a)



(b)

Fig. 4. (a) SEM image of a 2-D PBGF with core diameter of 21λ . Light gray disks are Ge-doped high-index inclusions. (b) Optical loss in a free fiber coil with a radius of 15 cm. Inset: near-field photograph of the fundamental mode at the output of a 10-cm-long straight fiber.

holes. Experimental data for bend sensitivity were available for the Bragg fiber, the 2-D PBGF, and the step-index fiber. The bending properties of LMA PCF were computed in [20] using the simple technique reported in [31]. The optical loss dependences via bend radius for different structures are presented in Fig. 5. It can be seen that the most bend-sensitive structure is the step-index fiber. Some reduction of the critical bend radius can be achieved by using a PCF or a 2-D solid-core PBGF. The Bragg fiber showed the smallest sensitivity to bending. Its critical bend radius (radius at which the bend loss is equal to 0.5 dB/m) is approximately two times smaller than that of the step-index fiber and 1.5 times smaller than that of the PCF and PBGF.

The possibility to reduce bend sensitivity in the PBGF by increasing Δn_{clad} was demonstrated earlier [25], [32]. In this paper, improvement of the structure with the core diameter of 43λ [21] was proposed. The new structure has the same core size Δn_{core} and the same distance between high-index layers, but

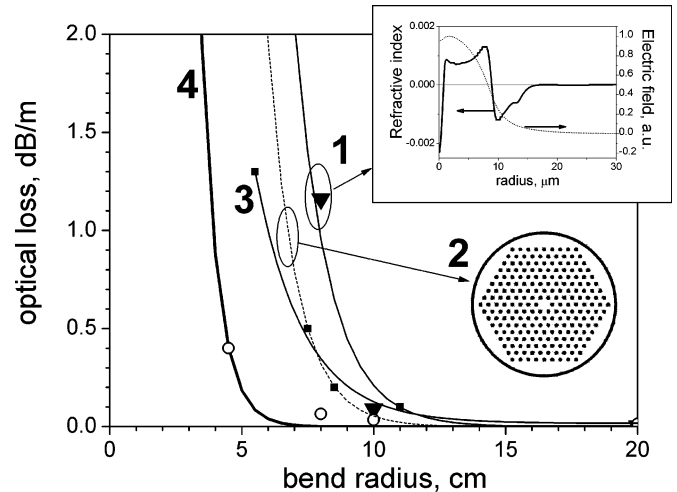


Fig. 5. Dependences of optical loss on bend radius for various types of fibers operating near $1.064 \mu\text{m}$ with mode-field diameter $\sim 19 \mu\text{m}$: 1—step-index fiber (RIP is shown in the inset); 2—PCF (cross section is shown in the inset); 3—2-D solid-core PBGF; 4—Bragg fiber.

the high-index layers were modified: a Δn_{clad} was increased from 0.010 to 0.030 together with corresponding reduction of the high-index layer thickness (to have the center of the bandgap at the same wavelength). The RIP of the resultant fiber and the optical loss measured for straight and bent fibers are shown in Fig. 6. Dependences of optical loss in the center of the bandgap ($1.2 \mu\text{m}$ for both fibers) on the bend radius are shown in Fig. 7. It can be seen that the losses in the straight and the bent fibers with $\Delta n_{\text{clad}} = 0.030$ are by more than an order of magnitude lower than that of fiber with $\Delta n_{\text{clad}} = 0.010$. The main problem of this technique is the reduction of optical loss of the high-order modes together with increasing of Δn_{clad} . A Bragg fiber shown in Fig. 6 becomes multimode at a few meters length.

A bend loss reduction caused by increasing Δn_{clad} was also reported for 2-D PBGF [33]. Contrary to the Bragg fibers, the confinement loss of such a structure becomes higher with increasing Δn_{clad} . A decrease of the diameter of the high-index cylinder required to keep bandgaps in the same place results in a decrease of the reflected area and explains the loss increase.

E. Comparison of Different Constructions of Solid-Core PBGF

Different LMA PBGF designs were discussed in this section. Comparing 1-D and 2-D PBGFs, we can conclude that the main advantage of the 2-D structure is the perfect single-modedness. On the other hand, Bragg fibers allow significant reduction in the size of the PBGF structure. Comparison of the various PBGF designs with mode-field diameter $\sim 19 \mu\text{m}$ shows that the Bragg fiber has the lowest bend sensitivity. Moreover, further bend sensitivity reduction is limited in Bragg fibers only by decreasing loss of the high-order modes. Techniques that allow improvement in single-modedness of the Bragg fibers are studied at the moment.

III. HIGH-POWER FIBER LASERS BASED ON ACTIVE PBGF

Unique properties of PBGF make them promising for high-power laser applications. Advantages of using PBGF for laser

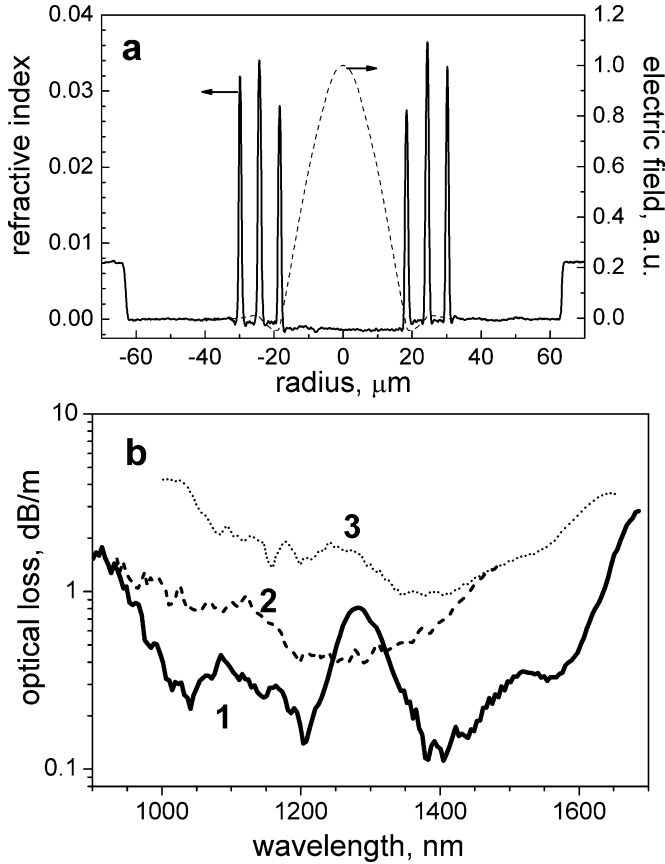


Fig. 6. (a) RIP in the Bragg fiber with a core diameter $D \sim 40\lambda$ and $\Delta n_{\text{clad}} = 0.030$ and the electric field distribution of the HE_{11} mode. (b) Optical loss measured in the straight (1) and bent fiber. The bend radius being 10 cm (2) and 5 cm (3). The peak in the loss spectra in the straight fiber is due to residual interference between the Bragg mirror and the polymer cladding.

applications were discussed in many papers, but only a few practical realizations have been described up to now. Early realizations use passive PBGFs [15], [16]. Recently, only two demonstrations of active PBGFs and lasers have been made [17], [34]. Such a situation was due to complexity of fabrication of active PBGF and some peculiarities of their use in fiber lasers. In this section, we discuss these problems and present recent results in this field.

A. Doping the Core With Rare-Earth Elements

The main problem of active PBGF fabrication is the necessity to keep the refractive index of the core at the level of pure silica or even below it. An increase of core refractive index can lead to additional light confinement due to total internal reflection and multimode propagation regime. On the other hand, the core of active fibers is usually doped with Al_2O_3 or P_2O_5 to prevent clustering of rare-earth ions. The doping level of Al_2O_3 or P_2O_5 should exceed the concentration of rare-earth ions in the core glass by a factor of 10 or even more [35]. Both of these oxides, Al_2O_3 or P_2O_5 , increase the refractive index of silica. As a result, fabrication of the core with a refractive index equal to that of pure silica and its doping by rare-earth ions with a concentration typical for usual active fibers become very

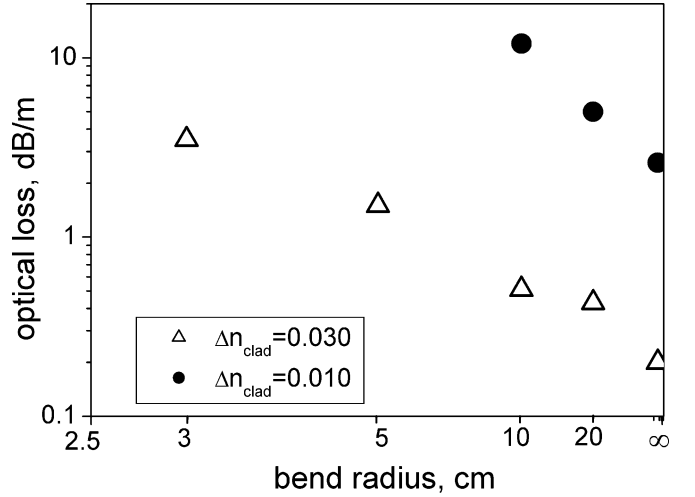


Fig. 7. Optical loss dependence on the bend radius in Bragg fibers with core diameter of about 40λ .

problematic. For this reason, in the first realization of active PBGF, the core index was 0.002 higher than that of pure silica, and direct pumping into the core was used owing to a small Yb^{3+} concentration [17]. The same problem takes place in the case of LMA air-silica-microstructured fibers, where only a large core to outer cladding ratio allows achieving high pump absorption from the cladding.

Additional core doping with fluorine solves this problem at least partially. Refractive index of silica could be decreased by fluorine codoping up to 0.010 [36]. However, fluorine codoping is difficult to use with Al- or P-doped silica. Al_2O_3 - SiO_2 and P_2O_5 - SiO_2 glasses heavily doped with fluorine have a rather low vitrification temperature that results in bubbling of the glass and evaporation of dopants during preform collapsing. Only 1 wt% of F (which corresponds to $\Delta n = -0.003$) can be incorporated into aluminosilicate and phosphorosilicate glasses easily. A further increase of the fluorine content requires modification of the technological process. Obtaining a uniform refractive index distribution in the core is also rather difficult in this case.

Another promising technique is the use of Al_2O_3 - P_2O_5 - SiO_2 ternary glasses. It was found earlier that the refractive index of silica codoped with Al_2O_3 and P_2O_5 in approximately equimolar amounts can be equal to or less than that of pure silica [37]. It has been shown recently that in a wide range of Al_2O_3 and P_2O_5 concentrations, it is possible to obtain low optical loss in such a host glass [38], [39]. The study of Yb-doped fibers based on this glass matrix has shown that together with a reduction of the numerical aperture, usage of the Al_2O_3 - P_2O_5 - SiO_2 ternary glasses allows one to decrease the photodarkening rate as compared to the traditional Yb-doped fibers with Al_2O_3 - SiO_2 core [40].

B. Highly Yb-Doped PBGF

In this paper [34], an active PBGF based on the 1-D structure, proposed in [20] (see also Fig. 2), was realized. This fiber was fabricated by the MCVD method and had a silica core doped

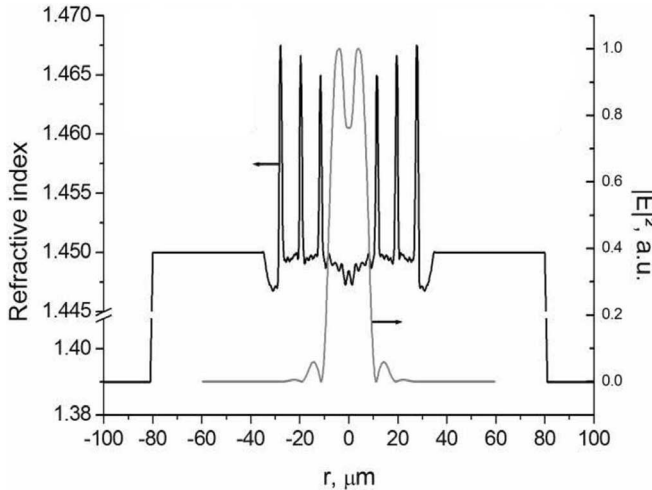


Fig. 8. RIP of the active Bragg fiber and the calculated electric field distribution of the HE₁₁ mode.

with Al₂O₃ and fluorine. A relatively high Yb³⁺ concentration (~1 wt%) was incorporated into the core from gas phase by use of metal-organic substances as a precursor. The RIP of the fiber fabricated is shown in Fig. 8. Variations of the core index by 0.0025 along radius were due to evaporation of the core dopants during preform collapsing. In the case of an LMA structure, these variations can significantly affect mode propagation. The mode characteristics (field distribution and confinement loss) were computed using the actual index profile in the assumption of infinite silica cladding. The confinement loss for high-order modes was found to be relatively high (~10 dB/m), as in the initial structure. The loss of the first mode increased from 0.01 [20] to ~1 dB/m owing to core index variations. The effective area of the fundamental mode was close to 200 μm².

The fiber was coated with a low-index polymer, the cladding numerical aperture being close to 0.48. As a result, light was confined in the core not only due to Fresnel reflection, but also owing to total internal reflection from the outer silica polymer cladding. Despite the fact that the calculated confinement loss of the high-order modes was relatively high in the case of an infinite silica cladding, these modes could propagate in the double-clad fiber. Observation of the transverse field intensity distribution at the output of a short (2 m) piece of fiber shows the presence of the first high-order TE₀₁ mode. As a result, an unpumped fiber is slightly multimode. A high optical loss in the case of an infinite silica cladding results in delocalization of light in the core of double-clad fiber. The share of the light power propagating in the Yb³⁺-doped region was computed to be 87% and 50% for the first and second modes, respectively. The appearance of selective amplification of modes and a quasi-single-mode behavior are expected in the case of pumped fiber.

C. Double-Clad Fiber Lasers Based on Active PBGF

A schematic of the experimental laser setup is shown in Fig. 9. Pump light was delivered by a multimode laser diode emitting at 975 nm with a pigtail core diameter of 100 μm and numerical aperture (NA) of 0.22. Due to the high Yb³⁺ concentration, a

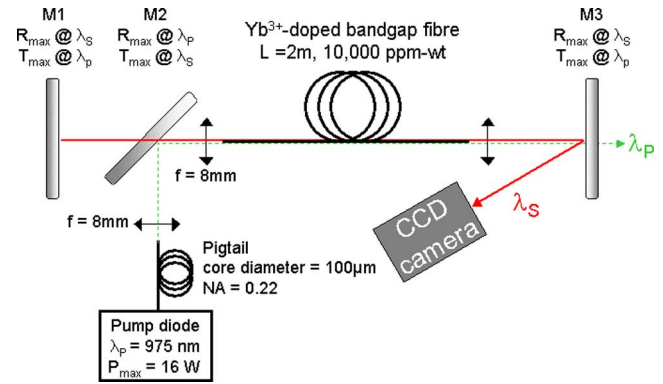


Fig. 9. Experimental setup of the cladding-pumped Yb³⁺-doped PBGF laser.

short piece of fiber (2 m) was used. The cavity mirrors were the dichroic mirror M1 with maximum reflectivity at the signal wavelength (R_{\max} @ 1060 nm) and the cleaved output end of the fiber. Launching of the pump power was carried out with a pair of 8-mm focal length collimating lenses. Launching efficiency reached 80%. The laser and unabsorbed pump beams were split at the output by using another dichroic mirror (M3, R_{\max} @ 1060 nm, T_{\max} @ 975 nm). It should be emphasized that any mechanical stress on the fiber should be avoided when maintaining the fiber on support plates. Otherwise, the index profile could be disturbed at the sites of mechanical strain and unwanted coupling to ring modes could occur.

First, the transverse distribution of the mode field intensity was observed at the output end of the laser. Circular symmetry of the beam profile shown in Fig. 10 allows one to assume that the emission is single mode. Single-modedness was also checked while shifting the output fiber in the transverse plane in front of the dichroic mirror M2. No high-order modes were observed in this case. The M^2 was measured by the knife-edge technique and was found to be equal to 1.17. It should be noted that light is confined in the low-index core, and the mode-field distribution is close to the Bessel function of the first kind and order (J_0). For this reason, the M^2 parameter obtained by comparing the emitted beam and pure Gaussian beam is slightly higher than that of the step-index fiber.

Next, the output power was measured as a function of the launched pump power for a straight active fiber. The results are plotted in Fig. 10. The slope efficiency was measured for the straight fiber to be 67% with respect to the launched power. Because of the circular outer cladding, the pump is not very efficiently absorbed in the fiber and the residual pump power decreases the slope efficiency. The slope efficiency with respect to the absorbed pump power was about 84%. Pump absorption can be improved, for instance, by using a D-shape inner cladding. Analysis of the output spectrum shows the presence of a number of laser lines typical for mirrors with a wide reflection spectrum.

Bend influence on lasing was also studied. The beam shapes were observed under several experimental conditions and are given in Fig. 11. Even for a very tight bend ($R_c = 7.5$ cm, seven turns), no high-order modes were excited. No influence on

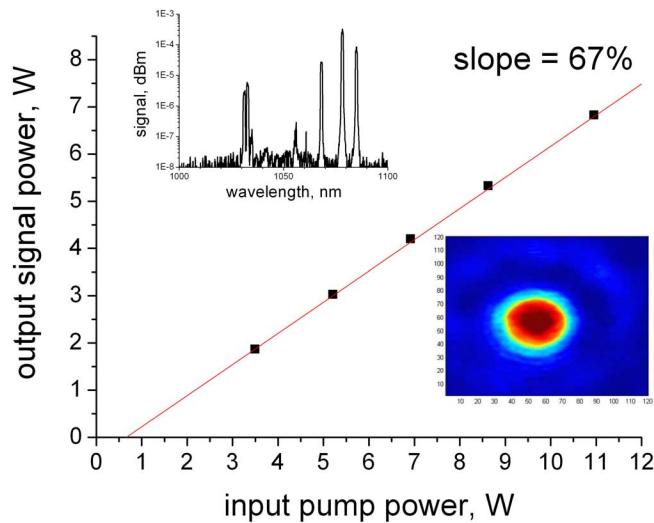


Fig. 10. Slope efficiency with respect to the launched pump power. Inset: measured emission spectrum and observed transverse distribution of the field intensity at the output of the 2-m-long straight fiber.

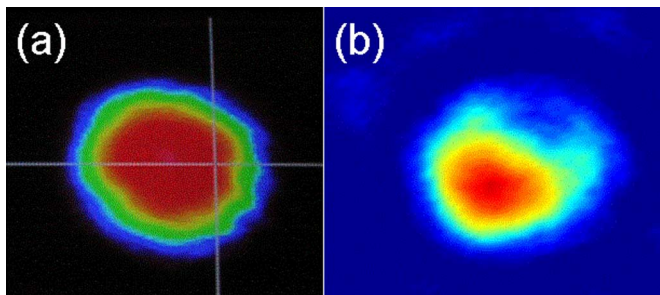


Fig. 11. Observed beam shapes under various experimental conditions. (a) $R_c = 7.5$ cm, three turns. (b) $R_c = 2.5$ cm, seven turns.

the beam shape was observed for $R_c = 7.5$ cm and three turns. Some localization of energy toward the exterior of the curvature occurs at $R_c = 2.5$ cm and seven turns. An increase of the lasing threshold (up to 6 W) and some decrease of the output power were found at this radius. At a 6-cm bend radius, neither variation of the slope efficiency nor the lasing threshold was observed.

An all-fiber laser based on the active PBGF was also tested [41]. A schematic of the laser setup is shown in Fig. 12(a). The pump with a central wavelength near 915 nm was coupled to a double-clad passive fiber with an outer diameter 125 μm and $\text{NA} = 0.4$. The pigtail fiber had a photosensitive core with a diameter of 20 μm and $\text{NA} = 0.06$. This fiber was spliced with an active Bragg fiber, 1.6 m in length. The laser cavity was formed by a Bragg grating with 100% reflectivity at 1.07 μm written in the pigtail fiber and a cleaved output Bragg fiber end with 4% reflectivity. The signal and the residual pump power were separated at the output and measured. Single-mode output was also obtained in this case. The output signal power was measured as a function of the absorbed pump power. The results are shown in Fig. 12(b). The slope efficiency is equal to 53%. A reduction of the efficiency as compared to the scheme with bulk elements is due to a high splicing loss between Bragg active

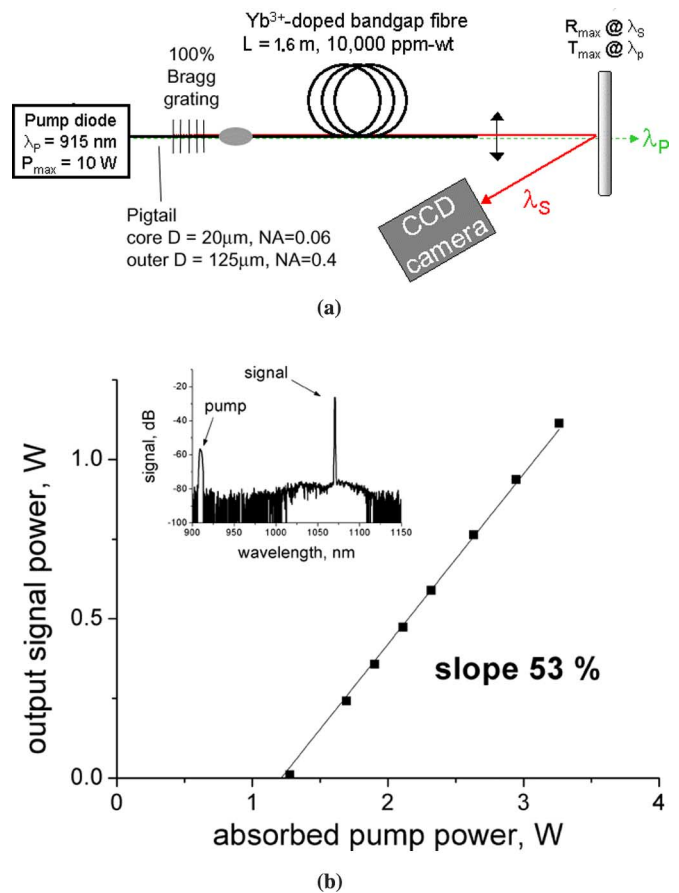


Fig. 12. (a) Experimental setup of an all-fiber cladding-pumped Yb³⁺-doped PBGF laser. (b) Slope efficiency measured with respect to the absorbed pump power. Inset: measured emission spectrum.

fiber and LMA step-index fiber (~ 1.6 dB), shorter fiber lengths, and a shorter pump wavelength.

IV. CONCLUSION

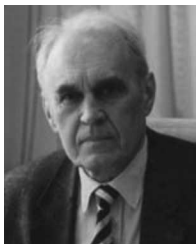
In conclusion, different LMA PBGF designs have been presented and discussed. Comparison of 1-D and 2-D PBGF shows that 1-D fibers allow one to reduce fiber size and bend sensitivity, whereas 2-D fibers have much better single-modedness. An increase of the core diameter up to 40λ and 32λ is possible in 1-D and 2-D designs, respectively.

The properties of active double-clad PBGFs and cladding-pumped fiber lasers based on such fiber have been analyzed. Single-mode output can be obtained in this case due to selective mode amplification despite the fact that a low-index polymer cladding suppresses the optical loss of high-order modes. A good beam quality was observed at a relatively high pump power. Above the threshold, the slope efficiency dependence versus the absorbed power reaches 84% in a scheme with bulk elements and 53% in an all-fiber scheme.

REFERENCES

- [1] K. P. Hansen, J. Broeng, P. M. W. Skovgaard, J. R. Folkenberg, M. D. Nielsen, A. Petersson, T. P. Hansen, C. Jakobsen, H. R. Simonsen, J. Limpert, and F. Salin, "High-power photonic crystal fiber lasers: Design, handling and subassemblies," presented at the Photon. West, San Jose, CA, 2005.

- [2] J. C. Knight, T. A. Birks, P. St. J. Russell, and D. M. Atkin, "All-silica single-mode optical fiber with photonic crystal cladding," *Opt. Lett.*, vol. 21, pp. 1547–1549, 1996.
- [3] J. Limpert, A. Liem, M. Reich, T. Schreiber, S. Nolte, H. Zellmer, A. Tünnermann, J. Broeng, A. Petersson, and C. Jakobsen, "Low-nonlinearity single-transverse-mode ytterbium-doped photonic crystal fiber amplifier," *Opt. Express*, vol. 12, pp. 1313–1319, 2004.
- [4] F. Röser, T. Eidam, J. Rothhardt, O. Schmidt, D. N. Schimpf, J. Limpert, and A. Tünnermann, "Millijoule pulse energy high repetition rate femtosecond fiber chirped-pulse amplification system," *Opt. Lett.*, vol. 32, pp. 3495–3497, 2007.
- [5] J. P. Kopolow, D. A. V. Kliner, and L. Goldberg, "Single-mode operation of a coiled multimode fiber amplifier," *Opt. Lett.*, vol. 25, pp. 442–444, 2000.
- [6] W. S. Wong, W. Peng, J. M. McLaughlin, and L. Dong, "Robust single-mode propagation in optical fibers with record effective areas," presented at the CLEO U.S., Baltimore, MD, 2005, Postdeadline Paper CPDB10.
- [7] S. Ramachandran, J. W. Nicholson, S. Ghalmi, M. F. Yan, P. Wisk, E. Monberg, and F. V. Dimarcello, "Light propagation with ultralarge modal areas in optical fibers," *Opt. Lett.*, vol. 31, pp. 1797–1799, 2006.
- [8] L. Lavoute, P. Roy, A. Desfarges-Berthelelot, V. Kermène, and S. Février, "Design of microstructured single-mode fiber combining large mode area and high rare earth ion concentration," *Opt. Express*, vol. 14, pp. 2994–2999, 2006.
- [9] P. Wang, L. J. Cooper, J. K. Sahu, and W. A. Clarkson, "Efficient single-mode operation of a cladding-pumped ytterbium-doped helical-core fiber laser," *Opt. Lett.*, vol. 31, pp. 226–228, 2006.
- [10] C.-H. Liu, G. Chang, N. Litchinister, D. Guertin, N. Jacobson, K. Tankala, and A. Galvanauskas, "Chirally coupled core fibers at 1550-nm and 1064-nm for effectively single-mode core size scaling," in *Proc. Conf. Lasers Electro-Opt./Quantum Electron. Laser Sci. Conf. Photonic Appl. Syst. Technol.*, (OSA Tech. Dig. Series (CD)) [Washington, DC: Optical Society of America], 2007, Paper CTuBB3.
- [11] Y. Chen, T. McComb, V. Sudesh, M. Richardson, and M. Bass, "Very large-core, single-mode, gain-guided, index-antiguidded fiber lasers" *Opt. Lett.*, vol. 32, pp. 2505–2507, 2007.
- [12] P. Yeh, A. Yariv, and E. Marom, "Theory of Bragg fiber," *J. Opt. Soc. Amer.*, vol. 68, pp. 1196–1201, 1978.
- [13] J. A. Argyros, T. A. Birks, S. G. Leon-Saval, C. M. B. Cordeiro, F. Luan, and P. St. J. Russell, "Photonics bandgap with an index step of one percent," *Opt. Express*, vol. 13, pp. 309–314, 2005.
- [14] F. Brechet, P. Roy, J. Marcou, and D. Pagnoux, "Singlemode propagation into depressed-core-index photonic-bandgap fibre designed for zero-dispersion propagation at short wavelengths," *Electron. Lett.*, vol. 36, pp. 514–515, 2000.
- [15] A. Isomaki and O. G. Okhotnikov, "All-fiber ytterbium soliton mode-locked laser with dispersion control by solid-core photonic bandgap fiber," *Opt. Express*, vol. 14, pp. 4368–4373, 2006.
- [16] A. Wang, A. K. George, and J. C. Knight, "Three-level neodymium fiber laser incorporating photonic bandgap fiber," *Opt. Lett.*, vol. 31, pp. 1388–1390, 2006.
- [17] L. Bigot, V. Pureur, G. Bouwmans, and Y. Quiquempois, "Ytterbium-doped 2D solid core photonic bandgap fiber for laser operation at 980 nm," presented at the 32th Eur. Conf. Opt. Commun., Berlin, Germany, Sep. 16–20 2007, Paper Mo 1.4.5.
- [18] S. G. Johnson, M. Ibanescu, M. Skorobogatiy, O. Weisberg, T. D. Engeness, M. Soljacic, S. A. Jacobs, J. D. Joannopoulos, and Y. Fink, "Low-loss asymptotically single-mode propagation in large-core OmniGuide fibers," *Opt. Express*, vol. 9, no. 13, pp. 748–779, 2001.
- [19] S. Février, P. Viale, F. Gerome, P. Leproux, P. Roy, J.-M. Blondy, B. Dussardier, and G. Monnom, "Very large effective area singlemode photonic bandgap fiber," *Electron. Lett.*, vol. 39, pp. 1240–1242, 2003.
- [20] S. Février, R. Jamier, J.-M. Blondy, S. L. Semjonov, M. E. Likhachev, M. M. Bubnov, E. M. Dianov, V. F. Khopin, M. Y. Salganskii, and A. N. Guryanov, "Low-loss singlemode large mode area all-silica photonic bandgap fiber," *Opt. Express*, vol. 14, pp. 562–569, 2006.
- [21] R. Jamier, P. Viale, S. Février, J. M. Blondy, S. L. Semjonov, M. E. Likhachev, M. M. Bubnov, E. M. Dianov, V. F. Khopin, M. Y. Salganskii, and A. N. Guryanov, "Depressed-index-core singlemode bandgap fiber with very large effective area," presented at the OFC/NFOEC Conf. 2006, Tech. Dig., Anaheim, CA.
- [22] Y. A. Uspenskii, E. E. Uzorin, A. V. Vinogradov, M. E. Likhachev, S. L. Semjonov, M. M. Bubnov, E. M. Dianov, R. Jamier, and S. Février, "Effect of polymer coating on leakage losses in Bragg fibers," *Opt. Lett.*, vol. 32, pp. 1202–1204, 2007.
- [23] D. A. Gaponov, A. S. Biriukov, A. D. Pryamikov, M. E. Likhachev, and S. Février, "Singlemodedness in Bragg fibers," presented at the Photonics 2008: Int. Conf. Fiber Opt. Photon., New Delhi, India, Dec. 13–17.
- [24] N. M. Litchinitser, S. C. Dunn, B. Usner, B. J. Eggleton, T. P. White, R. C. McPhedran, and C. M. de Sterke, "Resonances in microstructured optical waveguides," *Opt. Express*, vol. 11, pp. 1243–1251, 2003.
- [25] S. Février, R. Jamier, P. Viale, G. Humbert, F. Gerome, M. Devautour, L. Lavoute, P. Roy, J.-M. Blondy, S. L. Semjonov, M. E. Likhachev, M. M. Bubnov, E. M. Dianov, V. F. Khopin, M. Y. Salganskii, and A. N. Guryanov, "Solid-core bandgap fibers," presented at the Photon. West, San Jose, CA, 2007, vol. 6453, Invited Paper 64531A.
- [26] G. Bouwmans, L. Bigot, Y. Quiquempois, F. Lopez, L. Provino, and M. Douay, "Fabrication and characterization of an all-solid 2D photonic bandgap fiber with a low-loss region (< 20 dB/km) around 1550 nm," *Opt. Express*, vol. 13, pp. 8452–8459, 2005.
- [27] T. A. Birks, F. Luan, G. J. Pearce, A. Wang, J. C. Knight, and D. M. Bird, "Bend loss in all-solid bandgap fibres," *Opt. Express*, vol. 14, pp. 5688–5698, 2006.
- [28] A. Bétourné, V. Pureur, G. Bouwmans, Y. Quiquempois, L. Bigot, M. Perin, and M. Douay, "Solid photonic bandgap fiber assisted by an extra air-clad structure for low-loss operation around 1.5 μm ," *Opt. Express*, vol. 15, pp. 316–324, 2007.
- [29] O. N. Egorova, S. L. Semjonov, A. F. Kosolapov, A. N. Denisov, A. D. Pryamikov, D. A. Gaponov, A. S. Biriukov, E. M. Dianov, M. Y. Salganskii, V. F. Khopin, M. V. Yashkov, A. N. Gurianov, and D. V. Kuskonov, "Single-mode all-silica photonic bandgap fiber with 20- μm mode-field diameter," *Opt. Express*, vol. 16, pp. 11735–11740, 2008.
- [30] A. D. Pryamikov, A. S. Biriukov, D. A. Gaponov, O. N. Egorova, and S. L. Semjonov, "Optical properties of solid core photonic band gap fiber based on optical properties of single rod of its cladding," presented at the Photon. 2008: Int. Conf. Fiber Opt. Photon., New Delhi, India, Dec. 13–17.
- [31] M. D. Nielsen, N. A. Mortensen, M. Albertsen, J. R. Folkenberg, A. Bjarklev, and D. Bonaccini, "Predicting macrobending loss for large-mode area photonic crystal fibers," *Opt. Express*, vol. 12, pp. 1775–1779, 2004.
- [32] R. Jamier, S. Février, G. Humbert, M. Devautour, P. Viale, J.-M. Blondy, S. L. Semjonov, M. E. Likhachev, M. M. Bubnov, E. M. Dianov, V. F. Khopin, M. Y. Salganskii, and A. N. Guryanov, "Reduction of bend loss in large-mode-area Bragg fibres," in *Proc. SPIE*, 2007, vol. 6588, pp. 658804-1–658804-11, Paper 658805.
- [33] V. Pureur, A. Betourne, G. Bouwmans, L. Bigot, M. Douay, and Y. Quiquempois, "Bending losses in all solid 2D photonic band-gap fibers: A limiting factor?," in *Proc. 32th Eur. Conf. Opt. Commun.*, Cannes, France, Sep. 25–28, 2006, pp. 189–190, Paper We3.P.34.
- [34] S. Février, D. Gaponov, P. Roy, M. E. Likhachev, S. L. Semjonov, M. M. Bubnov, E. M. Dianov, M. Y. Yashkov, V. F. Khopin, M. Y. Salganskii, and A. N. Guryanov, "High-power photonic-bandgap fiber laser," *Opt. Lett.*, vol. 33, pp. 989–991, 2008.
- [35] K. Arai, H. Namikawa, K. Kumata, T. Honda, Y. Ishii, and T. Handa, "Aluminum or phosphorus co-doping effects on the fluorescence and structural properties of neodymium-doped silica glass," *J. Appl. Phys.*, vol. 59, pp. 3430–3436, 1986.
- [36] E. M. Dianov, M. V. Grekov, I. A. Bufetov, V. M. Mashinsky, O. D. Sazhin, A. M. Prokhorov, G. G. Devyatkykh, A. N. Guryanov, and V. F. Khopin, "Highly efficient 1.3 μm Raman fibre amplifier," *Electron. Lett.*, vol. 34, pp. 669–670, 1998.
- [37] D. J. DiGiovanni, J. B. MacChesney, and T. Y. Kometani, "Structure and properties of silica containing aluminum and phosphorus near the AlPO_4 join," *J. Non-Cryst. Solids*, vol. 113, pp. 58–64, 1989.
- [38] S. Unger, A. Schwuchow, J. Dellith, and J. Kirchhof, "Codoped materials for high power fiber lasers—Diffusion behaviour and optical properties," in *Proc. SPIE*, 2007, vol. 6469, p. 646913, Paper 646913.
- [39] D. S. Lipatov, M. V. Yashkov, A. N. Guryanov, M. E. Likhachev, K. V. Zotov, and M. M. Bubnov, "Optical properties of highly Al_2O_3 and P_2O_5 doped silica hosts for large mode area fiber lasers and amplifiers," presented at the 32th Eur. Conf. Opt. Commun., Berlin, Germany, Sep. 16–20, 2007, Paper P020.
- [40] S. Jetschke, S. Unger, A. Schwuchow, M. Leich, and J. Kirchhof, "Efficient Yb laser fibers with low photodarkening by optimization of the core composition," *Opt. Express*, vol. 16, pp. 15540–15545, 2008.
- [41] D. A. Gaponov, Optical Fiber Research Center of RAS, Moscow, Russian, Private Communication, Jan. 2008.



Evgeny M. Dianov (M'97) was born in Tula, Russia, on January 31, 1936. He received the Graduate degree from Moscow State University, Moscow, Russia, in 1960, and the Ph.D. degree and the Doctor of Science degree in physics and mathematics from P. N. Lebedev Physical Institute, Russian Academy of Sciences, Moscow, in 1966 and 1977, respectively.

Since 1994, he has been an Academician of the Russian Academy of Sciences, where he is currently the Director of the Fiber Optics Research Center. He has authored or coauthored more than 600 scientific

papers and patents. His current research interests include laser physics and fiber and integrated optics.

Dr. Dianov is a Fellow of the Optical Society of America and a member of the Material Research Society (MRS). He was the recipient of the State Prize of the Soviet Union in 1974 and the State Prize of Russia in 1998.



Sébastien Février was born in Périgord, France, in 1976. He received the Graduate degree in 1999 and the Ph.D. degree in 2002 from the University of Limoges, Limoges, France.

Since 2003, he has been an Associate Professor at Xlim Research Institute, University of Limoges, Limoges, France, where he has been engaged in research and development of optical fibers in the fields of fiber amplifiers, gain-flattening filters, and dispersion-compensating fibers. His current research interests include hollow and all-solid bandgap fibers

for high-power generation or delivery and management of nonlinear effects and dispersion properties as well as development of specialty fibers for midinfrared spectral domain.



Mikhail E. Likhachev was born in Moscow, Russia, in 1979. He received the Graduate degree from Moscow Institute of Physics and Technology, Moscow, in 2001, and the Ph.D. degree in laser physics from the General Physics Institute, Russian Academy of Sciences, Moscow, in 2005.

In 1999, he joined the Fiber Optics Research Center, Russian Academy of Sciences, where he is currently a Senior Fellow and engaged in research on optical loss mechanisms in highly germanium and phosphorous-doped fibers. His current research inter-

ests include study of photonic bandgap fibers and development of new materials for fiber lasers.